Scattering de electrones fuertemente interactuantes en nanotiras

Jorge Calvo Ibar

Advisors:
Luís Martín Moreno, Eduardo Sánchez Burillo y David Zueco Láinez

June 26, 2015

Contents

List of Figures

Chapter 1

Introduction

The aim of this work is to study the electronic transport and scattering in one-dimensional strips. The study of one-dimensional strips include many practical examples like the study of metalic nanowires, conducting polymers, graphene nanoribbons and among others. Also, we will study the electronic interaction between electrons and thes scattering in a small region of the lattice, known as Quantum Dot; using the tight-binding model shown in [4]. Nevertheless, we are not going to use the same procedure followed in [4]. We will develop a general procedure which will permit us to simulate the electronic transport for few electrons.

Figure 1.1: graphene nanoribbon (Figure obtained from [3]).

Due to the difficulty of the problem, we will need a numerical procedure which will require the discretization of our system or in other words we have to solve a many-body problem. But, as we will be able to see in the next sections, the number of parameters involved in the description of the system is too large to be represented in a "traditional way". To obtain a solution to this problem we will use the technique known as *Matrix Product States* or MPS [5] [6], a tensor network method which permits to represent quantum states in terms of networks of interconnected tensors.

This work will be divided in several sections: In the second chapter, we will develop all the theoretical tools which will allow us to deal with the physical problem of electronic propagation through one-dimensional lead, such as MPS representation of states and operators, the Suzuki-Trotter approximation for the time evolution, the truncation method which will permit to improve the efficiency of the simulation[1]...

After that introductory chapter, we will study, using the tight-biding model, the scattering of one electron against our Quantum Dot and we will obtain the ground state energies of our system with several electrons. Then we deal with the propagation of two electrons through the lattice. We will finish our work expressing the main conclusions and future projects in which the developed method can be applied.

[1] All the algorithms developed in this work will be done using MATLAB application.

Chapter 2

MPS and fermions

2.1 Matrix Product States (MPS), theoretical preliminaries

The challenge to understand the many-body problems which condensed matter physics provides, for example the high-T_c superconductivity [7], has provoked the emergence of many mathematical models which try to resolve them, as the Hubbard and $t-J$ models [8] (for the high-T_c superconductivity). However, this sort of problems involves many degrees of freedom. [5] So it is necessary a numerical approximate method to resolve them.

In order to ilustrate the problem of many dregrees of freedom supose if we try to represent a state $|\Psi\rangle$ in a lattice of N sites, where in every site there is a Hilbert space, with its own basis: $\{|i\rangle\}_{i=1}^{d_n}$. To represent $|\Psi\rangle$ in the complete Hilbert space, we have:

$$|\Psi\rangle = \sum_{i_1,\ \ldots i_N=1}^{d_1,\ \ldots,d_N} c_{i_1\ldots i_N}\,|i_1\ldots i_N\rangle \tag{2.1}$$

If every site has only two states and the number of sites is of the order of Avogadro number $N \sim 10^{23}$, we will need $\sim 2^{10^{23}}$ coefficients to represent only this state. This number is much bigger than the number of atoms in the observable universe which is stimated in 10^{80}.

There are many methods in the field of *Tensor Networks* to attack this kind of problems: Density Matrix Renormalization Group (DMRG), Tree *Tensor Networks* [6], Projected Entangled Pair States (PEPS) [5] [6]... But we are going to center our efforts on a particular method, the Matrix Product States (MPS) [5] [6].

Firstly, we have to explore the concept of rank-n tensor. For our purpose, a rank-n tensor can be described as a mathematical object with "n" indices; hence a rank-2 tensor is a matrix. The tensor could be drawn as a ball whose indices are lines emerging from it. The links represent the contractions between indices. Thus, a scalar product $C = \sum_{\alpha=1}^{D} A_\alpha B_\alpha$ will be represented by the connection of two indices.

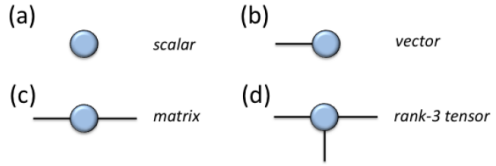

Figure 2.1: The different types of tensors [5].

Consequently, we can interpret the set of coefficients $c_{i_1\ldots i_N}$ as a rank-N tensor where every index corresponds to a site of our physical lattice. The numerical technique known as Matrix Products of States (MPS) consist on representing $c_{i_1\ldots i_N}$ as a one-dimensional *tensor network* where each site is occupied by a rank-3 tensor. So, instead of representing a very complex tensor it is more efficient, to use a network of simpler tensors. Thus, MPS representation is a technique which is adequate to represent a one-dimensional lattice. Every open index represents a physical degree of freedom of the Hilbert space and the connections between tensors are called virtual indices. We will see that all state $|\Psi\rangle$ can be described with a *tensor network* as a MPS.

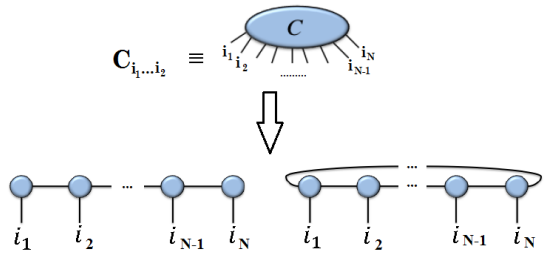

Figure 2.2: The MPS network of N sites, the left network has open boundary conditions and the right periodic boundary conditions (This image has been modified from others of [5]).

2.1.1 Single Value Decomposition (SVD)

We are going to see how we can decompose an arbitrary state $|\Psi\rangle$ in a MPS. The coefficients $c_{i_1 \ldots i_N}$ can be saved as a matrix $C_{i_1,\ (i_2 \ldots i_N)}$ grouping together the indices $i_2,\ \ldots,\ i_N$ as a unique index[1] . Besides, every matrix A $n \times m$ can be decomposed in three matrices through the single value decomposition [9]:

$$A = U\Sigma V^{\dagger}, \tag{2.2}$$

where U and V are unitary matrices with dimensions $n \times n$ and $m \times m$ respectively. The matrix Σ is a diagonal $n \times m$ matrix which entries are the singular values σ_i. This decomposition is applied over C:

$$C_{i_1,\ (i_2 \ldots i_N)} = \sum_{n_2=1}^{D_2} U_{i_1,n_2} \sigma_{n_2} V^{\dagger}_{(i_2,\ \ldots, i_N),n_2}, \tag{2.3}$$

where $D_2 = \min\{d_1,\ d_2 d_3 ... d_N\}$. So, we define $(A_1^{i_1})_{1,n_2} = U_{i_1,\ n_2}$ and $c'_{n_2,i_2,\ldots,i_N} = \sigma_{n_2} V^{\dagger}_{(i_2,\ldots,i_N),n_2}$. Therefore, the state is rewritten as:

$$|\Psi\rangle = \sum_{i_1,\ldots,i_N=1}^{d_1,\ldots,d_N} \sum_{n_2=1}^{D_2} (A_1^{i_1})_{1,n_2} c'_{n_2,i_2,\ldots,i_N} |i_1, ..., i_N\rangle \tag{2.4}$$

We can repeat the prosses and apply the single value decomposition, if we set $C'_{(n_2,i_2),(i_3,\ldots,i_N)} = c'_{n_2,i_2,\ldots,i_N}$:

$$C'_{(n_2,i_2),(i_3,\ldots,i_N)} = \sum_{n_3=1}^{D_3} U'_{(n_2,i_2)n_3} \sigma'_{n_3} V'^{\dagger}_{(i_3,\ldots,i_N),n_3} \tag{2.5}$$

Again $D_3 = \min\{D_2 d_2,\ d_3 d_4 ... d_N\}$ and we define $(A_2^{i_2})_{n_2,n_3} = U'_{(n_2,i_2)n_3}$ and $c''_{n_3,i_3,\ldots,i_N} = \sigma'_{n_3} V'^{\dagger}_{(i_3,\ldots,i_N),n_3}$. Therefore the state $|\Psi\rangle$ is:

$$|\Psi\rangle = \sum_{i_1,\ldots,i_N=1}^{d_1,\ldots,d_N} \sum_{n_2,n_3=1}^{D_2,D_3} (A_1^{i_1})_{1,n_2} (A_2^{i_2})_{n_2,n_3} c''_{n_3,i_3,\ldots,i_N} |i_1, ..., i_N\rangle \tag{2.6}$$

Repeating the process again and again we finally obtain:

$$|\Psi\rangle = \sum_{i_1,\ldots,i_N=1}^{d_1,\ldots,d_N} \sum_{n_2,\ldots n_N=1}^{D_2,\ldots,D_N} (A_1^{i_1})_{1,n_2} (A_2^{i_2})_{n_2,n_3} ... (A_{N-1}^{i_{N-1}})_{n_{N-1},n_N} (A_N^{i_N})_{n_N,1} |i_1, ..., i_N\rangle \tag{2.7}$$

As we have just seen, we can divide any rank-n tensor in "n" tensors $(A_j^{i_j})_{n_j,n_{j+1}}$, where i_j is the physical index and, n_j and n_{j+1} are the virtual indices. This is just a MPS whose representation is shown in figure 2.3. In other words, the tensor takes the place as the fundamental brick of the quantum state building $|\Psi\rangle$, as the DNA takes the place as the fundamental piece of life. This network of tensors offers, as we will see in the next sections, the opportunity to visualize the entanglement structure of $|\Psi\rangle$ and an efficient way to represent our state.

The rest of this section is mainly based on : [5]. In order to justify this representation we have to take into account that not all the states $|\Psi\rangle$ are of the same importance. The most typical Hamiltonians in nature are those which represent local interactions. This locality of the interactions implies that the low energy eigenstates follow the area

[1]Notice that each index i_j goes from $i_j = 1$ to $i_j = d_N$, where $j = 1, ..., N$

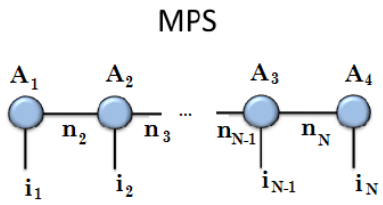

Figure 2.3: The MPS network with its indices (This image has been modified from others of [5]).

law of the entanglement entropy [10]. In other words the entanglement entropy grows as the area of the boundary and not as the volume like a random state. So, they are slightly entangled states. In addition, as we will see, this representation through MPS is a natural way which permits us to observe the entanglement structure of the state. If we consider the case of periodical conditions the final state is:

$$|\Psi\rangle = \sum_{i_1,\ldots,i_N=1}^{d_1,\ldots,d_N} \sum_{n_1,\ldots n_N=1}^{D_1,\ldots,D_N} (A_1^{i_1})_{n_1,n_2}(A_2^{i_2})_{n_2,n_3}\ldots(A_{N-1}^{i_{N-1}})_{n_{N-1},n_N}(A_N^{i_N})_{n_N,n_1}\,|i_1,\ldots,i_N\rangle, \tag{2.8}$$

where the different tensors are $(A_n^{i_n})_{m_n m_{n+1}}$, i_n is the physical index ("open" indices see figure 2.3) of n-site and m_n, m_{n+1} the virtual indices (links between sites). If we consider $d_i = d$ and $D_i = D$ for all $i = 1, \ldots, N$. Then, the number of parameters which codify the d^N coefficients are NdD^2, so, D must be an exponential number. Up until now, we have not done any approximation. First of all, we have to remember that D_i correspond to the number of singular values and some of them could be zero. So, we could reduce the dimension of our matrices to a smaller size χ_i. Notice that this new size matches with the rank of reduced density matrices between the subsystems of our network $\{1, \ldots, i\}$ and $\{i+1, \ldots, N\}$ [11] [12]. This quantity could be interpreted as a measure of the entanglement between both regions. If χ_i were equal to 1, then, our state could be represented by a tensor product between the two parts [2]. Therefore, the entanglement between both subsystems would be absent and if the dimension increased, the entanglement would increase too.

On the other hand, if the values of the D_i singular values present a great decay, we could approximate our calculus and reduce the number of coefficients (NdD^2), and thus improve the efficiency of the numerical method. In this case we could truncate our matrices and reduce the calculus time. In other words, when we want to represent a low-energy eigenstate we can truncate it due to its low entanglement.

Another way to see that D_i is a measure of entanglement between tensor neighbours, it is the following example: imagine a state represented as a two-dimensional *tensor network* (PEPS) [5] [6], as we show in the figure 2.4 (b). The size of the network side is L and if we call $\bar{\alpha} = \{\alpha_1, \ldots, \alpha_{4L}\}$ the combined index of the boundary, we can represent this state as the tensor product between the inner and outer state:

$$|\Psi\rangle = \sum_{\bar{\alpha}=1}^{D^{4L}} |in(\bar{\alpha})\rangle \otimes |out(\bar{\alpha})\rangle \tag{2.9}$$

Where the reduced density matrix of the inner part is:

$$\rho_{in} = \sum_{\bar{\alpha},\bar{\alpha}'=1}^{D^{4L}} \chi_{\bar{\alpha}\bar{\alpha}'}\,|in(\bar{\alpha})\rangle \otimes \langle in(\bar{\alpha}')|\,, \tag{2.10}$$

with $\chi_{\bar{\alpha}\bar{\alpha}'} \equiv \langle out(\bar{\alpha}')|out(\bar{\alpha})\rangle$. Notice that its maximum rank would be D^{4L}, if every virtual index were $\alpha_i = D$. Then, it can be demonstrated that the entanglement entropy $S(L) = -tr(\rho_{in}\log\rho_{in})$ [10] [13](von Neumann entropy) is limited by the logarithm of the reduced density matrix rank:

$$S(L) \leqslant 4L\log D \tag{2.11}$$

[2]Or in other words: $|\Psi\rangle = |\Psi_{\{1,\ldots,i\}}\rangle \otimes |\Psi_{\{i+1,\ldots,N\}}\rangle$

In other words, the entanglement entropy follows the area law. The entanglement "grows" (it is upper bounded) as the boundary area, which means, a greater network implies bigger entropy and therefore a bigger entanglement. Furthermore, notice that each connection contribute to the entropy as $\log D$. So, there are two main contributions to the entropy the area of the boundary and the "weight" of the virtual indices of the lattice (the size of D). Therefore, as we have seen, the *tensor network*s are the natural language to visualize the entanglement structure of every state.

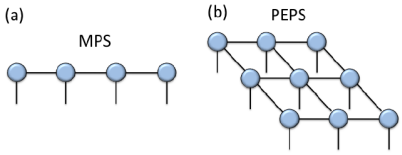

(a) The one-dimensional *Tensor Network* (MPS) and the two-dimensional *Tensor Network* [5].

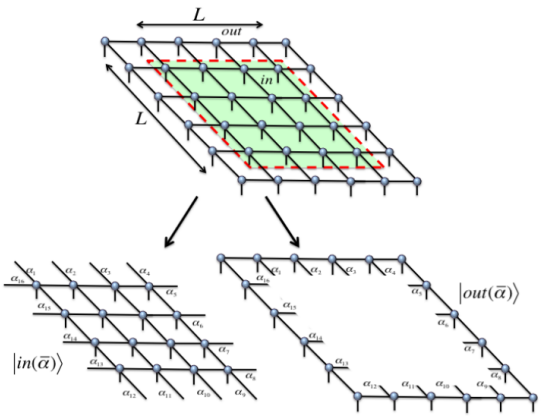

(b) Example of a PEPS network which form is a square with side L.

Figure 2.4: Projected Entangled Pair States (PEPS) a two-dimensional tensor network. [5]

2.1.2 Expected values and Matrix Product Operator (MPO)

The next question is how we can obtain the expected value of a specific operator using MPS language. Firstly we have to notice that every operator can be decomposed in a sum of tensor product of local operators: $O = O_1 \otimes O_2 \otimes \cdots \otimes O_N$, where every operator O_j is a local operator of the Hilbert space corresponding to the j-site. The first step to obtain the matrix element of O operator between the states $|\psi\rangle$ and $|\phi\rangle$ is to represent them as a MPS network:

$$|\psi\rangle = \sum_{\{i_n\}} A_1^{i_1} \dots A_N^{i_N} \, |i_1 ... i_N\rangle \tag{2.12}$$

$$|\phi\rangle = \sum_{\{j_n\}} B_1^{j_1} \dots B_N^{j_N} \, |j_1 ... j_N\rangle \tag{2.13}$$

If we take into account these last equations, we obtain:

$$\begin{aligned}
\langle\psi|O|\phi\rangle \quad &= \sum_{\{i_n, j_n\}} (A_1^{i_1} \dots A_N^{i_N})^* (B_1^{j_1} \dots B_N^{j_N}) \, \langle i_1|O_1|j_1\rangle \dots \langle i_N|O_N|j_N\rangle = ... \\
... \quad &= \sum_{\{i_n, j_n\}} ((A_1^{i_1})^* \otimes B_1^{j_1})((A_2^{i_2})^* \otimes B_2^{j_2}) \dots ((A_N^{i_N})^* \otimes B_N^{j_N})(O_1)_{i_1 j_1} \dots (O_N)_{i_N j_N} = ... \\
... \quad &= \prod_{n=1}^{N} \sum_{\{i_n j_n\}} (O_n)_{i_n j_n} ((A_n^{i_n})^* \otimes B_n^{j_n}),
\end{aligned}$$

where $(O_n)_{i_n j_n} = \langle i_n|O_n|j_n\rangle$ and remembering that the connections between indices represent the contractions of our tensors, we can represent our expected value as it is shown in *figure 2.5*.

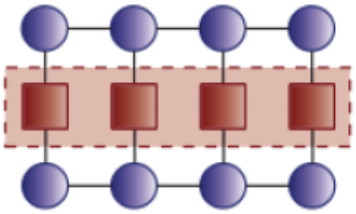

Figure 2.5: MPS representation of expected value of operator O (Figure obtained from [16]).

All this section about Matrix Product Operator is mainly based on reference [14]. However this procedure is not as efficient as we desired in some cases. We could represent our operator in a similar way as our state was represented using MPS scheme. This scheme is known as Matrix Product Operator (MPO). For example consider the following operator:

$$O = \sum_{\{i_n\}\{j_n\}} c_{i_1,j_1,i_2,j_2,\ldots,i_N,j_N} \left|i_1,\ldots,i_N\right\rangle \left\langle j_1,\ldots,j_N\right| \tag{2.14}$$

So, as we have done, we could interpret our set coefficients $c_{i_1,j_1,i_2,j_2,\ldots,i_N,j_N}$ as a tensor network where in each site has a rank-four tensor. Hence, using the single value decomposition in a similar way as MPS case, this operator O can be decomposed as:

$$O = \sum_{\{i_n\}\{j_n\}} C_1^{i_1 j_1} \ldots C_N^{i_N j_N} \left|i_1,\ldots,i_N\right\rangle \left\langle j_1,\ldots,j_N\right| \tag{2.15}$$

It is easy to see that this MPO acting on an MPS produces a MPS again. But, is it easy to write any operator as MPO? The sum of one and two-site operator are tractable cases which are relatively simple. For instance in the case of a sum of one-site operators $O = \sum_{n=1}^{N} X_n$, it can be shown that the matrices of MPO representation are:

$$C_1^{i_1 j_1} = \begin{pmatrix} (X_1)_{i_1 j_1} & \delta_{i_1 j_1} \end{pmatrix} \qquad C_n^{i_n j_n} = \begin{pmatrix} \delta_{i_n j_n} & 0 \\ (X_n)_{i_n j_n} & \delta_{i_n j_n} \end{pmatrix} \qquad C_N^{i_N j_N} = \begin{pmatrix} \delta_{i_N j_N} \\ (X_N)_{i_N j_N} \end{pmatrix}, \tag{2.16}$$

where $(X_n)_{i_n j_n} = \langle i_n | X_n | j_n \rangle$. Equivalently for the case of sum of two-site operators: $O = \sum_{n=1}^{N} X_n Y_{n+1}$, where X_n and Y_n are one-site operators, the matrices of MPO decomposition are:

$$C_1^{i_1 j_1} = \begin{pmatrix} 0 & (X_1)_{i_1 j_1} & \delta_{i_1 j_1} \end{pmatrix} \qquad C_n^{i_n j_n} = \begin{pmatrix} \delta_{i_n j_n} & 0 & 0 \\ (Y_n)_{i_n j_n} & 0 & 0 \\ 0 & (X_n)_{i_n j_n} & \delta_{i_n j_n} \end{pmatrix} \qquad C_N^{i_N j_N} = \begin{pmatrix} \delta_{i_N j_N} \\ (Y_N)_{i_N j_N} \\ 0 \end{pmatrix} \tag{2.17}$$

This can be used in many different cases. For instance, it is very useful to build an initial state or the Hamiltonian of our system if we only have an operator based on a sum of one or two-body operators, as we will develop in the next sections. When, we talk about "initial state". We refer to build the initial conditions to propagate one, two, three... excitations. In these cases, we have to apply operators[3] like: $O = \sum_n^N c_n \sigma_n^+$, where c_n could be a wave packet $c_n = e^{-\frac{(n-X_o)^2}{2\sigma^2}} e^{-iK_o n}$ ([4]), several times over $|0...0\rangle$ the state of zero excitations. So, we can apply the MPO representation over O and then apply it over the MPS of $|0...0\rangle$.

[3] In the case of a one dimensional lattice of N sites.

[4] Where σ^+ is the spin creation operator (each site can only have one or zero excitations), X_o mean position and K_o mean momentum.

2.2 Time evolution

This section is divided in two subsections. The first is the Suzuki-Trotter decomposition and the second the imaginary time evolution. These are mainly based on the reference [15].

2.2.1 Suzuki-Trotter decomposition

Given a Hamiltonian $\mathscr{H}$ which can be expressed as a sum of operators of one and two-site operators:

$$\mathscr{H} = \sum_{i=1}^{N} h_i + \sum_{i=1}^{N-1} h_{i,i+1}, \tag{2.18}$$

where h_i is an operator which acts on the site "i" and $h_{i,i+1}$ acts on the site "i" and "$i+1$". It is necessary to know how we can implement the time evolution operator $U(t)$ to a state expressed as MPS, $U(t)\left|\psi\right\rangle = e^{-iHt}\left|\psi\right\rangle$ (where $\hbar = 1$) Due to technical reasons we are going to need some approximations. Firstly, notice that we can rewrite our Hamiltonian as:

$$\mathscr{H} = \underbrace{\boxed{\sum_{i=1}^{N/2} h_{2i} + \sum_{i=1}^{N/2-1} h_{2i,2i+1}}}_{H_E} + \underbrace{\boxed{\sum_{i=1}^{N/2} h_{2i-1} + \sum_{i=1}^{N/2} h_{2i-1,2i}}}_{H_O}, \tag{2.19}$$

where H_E and H_O are the even and odd operators respectively. Also, we have to notice that $h_{2i} + h_{2i,2i+1}$ commute among themselves. Since, for example, the two operators: $h_2 + h_{2,3}$ and $h_4 + h_{4,5}$ belong to different Hilbert spaces $H_2 \otimes H_3$ and $H_4 \otimes H_5$. If Hamiltonian were $\mathscr{H} = H_E$, the time evolution would be:

$$e^{-iH_E t}\left|\psi\right\rangle = \left(\prod_{n=1}^{N/2-1} e^{-i(h_{2n}+h_{2n,2n+1})t} e^{-ih_N t}\right)\left|\psi\right\rangle \tag{2.20}$$

Then, we only apply one and two-body operators which conserve the MPS scheme with a larger value of bond dimension. It can be shown that we can approximate temporal evolution operator $U(t) = \exp(-i\mathscr{H}\delta t) = \exp(-i(H_E + H_O)\delta t) \approx \exp(-iH_E\delta t)\exp(-iH_O\delta t) + o((\delta t)^2)$. This approximation is known as Suzuki-Trotter approximation of order 2 which we will use successively when we will build the time evolution operator $U(t)$ to propagate our fermi excitations through the lattice. There are other versions of order 3 and 5:

$$\exp(-i(H_E + H_O)\delta t) \approx \exp(-iH_E\delta t/2)\exp(-iH_O\delta t)\exp(-iH_E\delta t/2) + o((\delta t)^3) \tag{2.21}$$

$$\begin{aligned}\exp(-i(H_E + H_O)t) \approx \quad & \exp(-iH_E\theta\delta t/2)\exp(-iH_O\theta\delta t)\exp(-iH_E(1-\theta)\delta t/2)\exp(-iH_O(1-2\theta)\delta t)\times\ldots \\ & \cdots\times\exp(-iH_E(1-\theta)\delta t/2)\exp(-iH_O\theta\delta t)\exp(-iH_E\theta\delta t/2) + o((\delta t)^5)\end{aligned}$$

So, we have obtained an approximation which preserves the MPS representation due to successive application of one and two-body operators.

2.2.2 Imaginary time evolution

We are going to see a method known as imaginary time evolution which is going to allow us to obtain the ground state of our system. First of all we need to decompose our state $\left|\psi(0)\right\rangle$ as a sum of eigenstates of the Hamiltonian $\{\left|\phi_n\right\rangle\}$:

$$\left|\psi(0)\right\rangle = \sum_n c_n \left|\phi_n\right\rangle \tag{2.22}$$

Now to obtain the state $\left|\psi(t)\right\rangle$ we have to apply the time evolution operator $\exp(-i\mathscr{H}t)$, but we are going to substitute $t = -i\tau$, with τ belonging to positive real numbers. Hence, the final result is:

$$\left|\psi(\tau)\right\rangle = \sum_n c_n e^{-E_n\tau}\left|\phi_n\right\rangle, \tag{2.23}$$

where $\{E_n\}$ are the eigenvalues of the eigenstates basis $\{\left|\phi_n\right\rangle\}$.

They are arranged in a rising order $\{E_0 < E_1 < E_2 < \dots\}$. So, if we define the state $|\Psi(t)\rangle$, we obtain:

$$|\Psi(\tau)\rangle = \frac{|\psi(\tau)\rangle}{\sqrt{\langle\psi(\tau)|\psi(\tau)\rangle}} = \frac{\sum_n c_n e^{-E_n\tau}}{\sqrt{\sum_l |c_l|^2 e^{-2E_l\tau}}} \tag{2.24}$$

Taking the limit $\tau \longrightarrow +\infty$ the only surviving term is the ground state one $|\phi_0\rangle$:

$$\lim_{\tau\longrightarrow+\infty} |\Psi(\tau)\rangle = \frac{c_0\,|\phi_0\rangle}{|c_0|} \tag{2.25}$$

Therefore this method permits to obtain the ground state, its energy and other properties.

2.3 Truncation Method

This section and the appendix A has been based on Eduardo Sánchez Burillo's master thesis [16], one of the advisor of this work, and it has been inserted here with the consent of the advisers.

As we have said in before sections, we need to truncate the virtual indices of our MPS representation to develop all the potential of MPS language in order to obtain a equivalent network of smaller tensor which will improve the speed and efficiency of the simulation, and reducing memory necessary to do it. This problem consist on minimise the distance between the initial state $|\Psi\rangle$ with an MPS representation whose tensors are A_n and a generic one with smaller tensors $|\Phi\rangle$ whose tensors are B_n. In other words, we have to minimize:

$$d^2(|\Psi\rangle, |\Phi\rangle) = (\langle\Psi| - \langle\Phi|)(|\Psi\rangle - |\Phi\rangle) = 1 + \langle\Phi|\Phi\rangle - 2\mathrm{Re}(\langle\Psi|\Phi\rangle) \tag{2.26}$$

Now, we need to minimize the last equation with respect to $|\Phi\rangle$. To do that task, we start by minimising B_1 the tensor of the first site of the lattice and the rest of tensors of the other sites of lattice remain constant. Then, we can continue interatively minimising respect to B_2 and remain constant the rest and so on. On the other hand, in the case of minimising B_n, if v_n^Ψ and v_n^Φ are the vectorisations of A_n and B_n, as we will show in the appendix A, we need to minimise the following quadratic form:

$$f(A_n, B_n) = 1 + (v_n^\Phi)^\dagger E_1 v_n^\Phi - 2\mathrm{Re}\left((v_n^\Psi)^\dagger E_2 v_n^\Phi\right), \tag{2.27}$$

where E_1 and E_2 are matrices depending on the rest of tensors. Note that f is the scared of de distance between $|\Psi\rangle$ and $|\Phi\rangle$, but its variables are only the tensors linked to the site n. The quadratic form is minimised when v_n^Φ obeys the following system of linear equations (the proof is omitted because it is trivial):

$$E_1 v_n^\Phi = E_2^\dagger v_n^\Psi \tag{2.28}$$

When we have minimized with respect each tensor B_n up to the end of the chain, we can start the process again (but in inverse order), until we achieved the convergence. One possible convergence criteria could be that our distance takes a value smaller than a predetermined value of tolerance. All the information referred to the truncation method can be found in the appendix A.

2.4 Fermions

During this chapter we have seen a brief overview about the advantages of MPS representation. Secondly, we have shown that every state can be represented using this language and how the MPO representation can help us to obtain the expected values. Thirdly the Suzuki-Trotter approximation and imaginary time evolution taught us how to get the time evolution and the ground state of the system and finally the truncation procedure explains us how to reduce the "size" of our problem in order to make easier our numerical calculus. However, this is valid for spin and bosonic systems, but not for fermions, but we are interested in fermionic problems in this work. So, we will have to take into account that the fermionic creation/annihilation operators (f_n, f_m^+) follow the anticommutation relations:

$$\{f_n, f_m^+\} = \delta_{nm} \qquad \{f_n, f_m\} = 0 \tag{2.29}$$

2.4.1 Jordan-Wigner

So, we need a rule which permits us to change from fermionic to spin operators and vice versa. This is the Jordan-Wigner transformation:

$$\sigma_n^+ \equiv e^{-i\pi \sum_{l=1}^{n-1} f_l^+ f_l} f_n^+ \qquad \sigma_n^- = (\sigma_n^+)^+ \tag{2.30}$$

It can be shown that the inverse transformation is the following:

$$f_n^+ = e^{-i\pi \sum_{l=1}^{n-1} \sigma_l^+ \sigma_l^-} \sigma_n^+ \qquad f_n = (f_n^+)^+, \tag{2.31}$$

where $f's$ and $\sigma's$ are the fermionic and bosonic operators respectively. Notice that in a spin lattice each site can only have one or zero bosonic excitation. So, with the basis $\{|0\rangle, |1\rangle\}$, the operators $\sigma_n^+,\ \sigma_n^-$ are:

$$\sigma_n^+ = \begin{pmatrix} 0 & 0 \\ 1 & 0 \end{pmatrix} \qquad \sigma_n^- = \begin{pmatrix} 0 & 1 \\ 0 & 0 \end{pmatrix} \tag{2.32}$$

Also, it can be shown that the bosonic operators follow the next commutation and anticommutation relations:

$$[\sigma_n^-, \sigma_m^-] = 0 \qquad [\sigma_n^-, \sigma_m^+] = -\delta_{nm}(2\sigma_n^+ + \sigma_n^- - 1) \qquad \{\sigma_n^-, \sigma_m^+\} = \delta_{nm} \tag{2.33}$$

So, applying the rules shown before the $f_n^+ f_m^+$ can be written in terms of spin operators as:

$$\begin{aligned} f_n^+ f_m^+ &= \sigma_n^+ \exp\left(i\pi \sum_{l=1}^{n-1} \sigma_l^+ \sigma_l^-\right) \exp\left(i\pi \sum_{l=1}^{m-1} \sigma_l^+ \sigma_l^-\right) \sigma_n^+ = \sigma_n^+ \exp\left(i2\pi \sum_{l=1}^{n-1} \sigma_l^+ \sigma_l^- + i\pi \sum_{l=1}^{m-1} \sigma_l^+ \sigma_l^-\right) \sigma_m^+ \\ &= \sigma_n^+ \exp\left(i\pi \sum_{l=n}^{m-1} \sigma_l^+ \sigma_l^-\right) \sigma_m^+ \end{aligned} \tag{2.34}$$

Another interesting expression which we will show (and use) in the next sections is:

$$f_n^+ f_n = \sigma_n^+ \sigma_n^- \tag{2.35}$$

This method we will permit us to develop a fermionic problem like a spin problem. Then, it can permit us to use the simple operators (2.32), instead of their fermionic equivalents.

Chapter 3

Physical problem and results

3.1 Tight-binding model

In the last chapter we have explained the MPS method. So, we can now apply this technique to several physical problems of electron propagation. Then we will see interacting systems but first we have to check the validity of our method with easier models. We are going to start with the simplest model to study the electron transport along a one-dimensional chain, the tight-binding model. Imagine a chain of N sites with free boundary conditions and with a hopping constant between sites J:

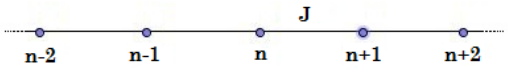

Figure 3.1: Chain of N sites with an exchange J.

The Hamiltonian which describes our model is:

$$\mathscr{H} = E_o \sum_{n=1}^{N} f_n^+ f_n + J \sum_{n=1}^{N-1} \left(f_n^+ f_{n+1} + f_{n+1}^+ f_n \right) \tag{3.1}$$

Firstly, we are going to solve our Hamiltonian. To diagonalize it, we need to use the Fourier transform to pass to the momentum space:

$$\hat{f}_k = \frac{1}{\sqrt{N}} \sum_{j=1}^{N} e^{ikj} f_j \;\longrightarrow\; f_j = \frac{1}{\sqrt{N}} \sum_{k=1}^{N} e^{-ikj} \hat{f}_k \tag{3.2}$$

$$\hat{f}_k^+ = \frac{1}{\sqrt{N}} \sum_{j=1}^{N} e^{-ikj} f_j^+ \;\longrightarrow\; f_j^+ = \frac{1}{\sqrt{N}} \sum_{k=1}^{N} e^{ikj} \hat{f}_k^+ \tag{3.3}$$

Apart from these equations we will have in mind the fermion anticommutation relations:

$$\{\hat{f}_k,\ \hat{f}_{k'}^+\} = \delta_{kk'} \quad \{\hat{f}_k,\ \hat{f}_{k'}\} = 0 \quad \{\hat{f}_k^+,\ \hat{f}_{k'}^+\} = 0 \tag{3.4}$$

Substituting these last equations in the Hamiltonian $\mathscr{H}$, we obtain:

$$\mathscr{H} = \frac{1}{N} \sum_{j=1}^{N} \left[E_o \sum_{kk'}^{N} \left(\hat{f}_k^+ \hat{f}_{k'} e^{i(k-k')j} \right) + J \sum_{kk'}^{N} \left(\hat{f}_{k'}^+ \hat{f}_k e^{i(k'j-k(j+1))} + \hat{f}_{k'}^+ \hat{f}_k e^{i(k'(j+1)-kj)} \right) \right] =$$

$$= \frac{1}{N} \left\{ \sum_{kk'}^{N} E_o \hat{f}_k^+ \hat{f}_{k'} \sum_{j=1}^{N} e^{i(k-k')j} + J \sum_{kk'}^{N} \hat{f}_{k'}^+ \hat{f}_k e^{-ik} \sum_{j=1}^{N} e^{i(k'-k)j} + J \sum_{kk'}^{N} \hat{f}_{k'}^+ \hat{f}_k e^{ik'} \sum_{j=1}^{N} e^{i(k'-k)j} \right\} = \dots$$

In the following we take into account that $N \gg 0$. It can be shown that $\sum_{j=1}^{N} e^{i(k-k')j} = N\delta(k-k')$ [1]. So, using this expression, we can continue our calculus:

$$\ldots = \frac{1}{N}\left\{ \sum_{kk'}^{N} E_o \hat{f}_k^+ \hat{f}_{k'} N\delta(k-k') + J\sum_{kk'}^{N} \hat{f}_{k'}^+ \hat{f}_k e^{-ik} N\delta(k'-k) + J\sum_{kk'}^{N} \hat{f}_{k'}^+ \hat{f}_k e^{ik'} N\delta(k'-k) \right\} =$$

$$= \sum_{k=1}^{N} \left[E_o \hat{f}_k^+ \hat{f}_k + J(\hat{f}_k^+ \hat{f}_k e^{-ik} + \hat{f}_k^+ \hat{f}_k e^{ik}) \right] = \sum_{k=1}^{N} \left[E_o \hat{f}_k^+ \hat{f}_k + 2J\hat{f}_k^+ \hat{f}_k \left(\frac{e^{ik} + e^{-ik}}{2} \right) \right] + J\sum_{k=1}^{N} e^{-ik} =$$

$$= \sum_{k=1}^{N} \left[E_o \hat{f}_k^+ \hat{f}_k + 2J\hat{f}_k^+ \hat{f}_k \cos(k) \right] + JN\delta(1) = \sum_{k=1}^{N} \left[(E_o + 2J\cos(k))\hat{f}_k^+ \hat{f}_k \right]$$

Hence the diagonalized Hamiltonian is:

$$\boxed{\mathscr{H} = \sum_{k=1}^{N} E_k \hat{f}_k^+ \hat{f}_k}, \text{ where } E_k = E_o + 2J\cos(k). \tag{3.5}$$

Now, if we consider the next state:

$$\boxed{|\Psi\rangle = (\hat{f}_{k_1}^+)^{n_1} (\hat{f}_{k_2}^+)^{n_2} \ldots (\hat{f}_{k_N}^+)^{n_N} |00\ldots00\rangle}, \text{ where } n_j = 0,\ 1 \quad \forall j = 1, ..., N \tag{3.6}$$

If our Hamiltonian $\mathscr{H}$ acts over $|\Psi\rangle$ each pair of operators $\hat{f}_{k_j}^+ \hat{f}_{k_j}$ only acts over its correspondent Hilbert space of the momentum k_j. So, when $n_j = 0$ there are not fermions with that momentum k_j. Hence, this pair does not contribute to the sum. Nevertheless, if $n_j = 1$, there are one fermion and $\hat{f}_k^+ \hat{f}_k |1\rangle = |1\rangle$. Therefore:

$$\mathscr{H}|\Psi\rangle = \left(\sum_{i=1}^{N} n_i E_{k_i} \right) |\Psi\rangle \text{, where } n_i \text{ corresponds to the number of fermions (1 or 0) with momentum "}k_i\text{".} \tag{3.7}$$

Hence the ground state energy E_{GS} is:

$$\boxed{E_{GS} = \sum_{k\in C} \left[E_o + 2J\cos(k) \right]}, \tag{3.8}$$

where we have summed over the k's which minimized the energy and the number of addends is the total number of fermions in our state at the beginning of the simulation.

Thus, our set of states $|\Psi\rangle$ are the eigenstates of the Hamiltonian $\mathscr{H}$ with eigenvalues $\sum_{i=1}^{N} n_i E_{k_i}$, $\forall$ set $\{n_i\}$. Now, once we have just diagonalize our Hamiltonian. We are going to obtain the allowed values of k, if we apply closed boundary conditions[2]. In other words, we are going to study the case of a chain of "N" sites. Suppose that we have a one-excitation quantum fermionic state:

$$|\psi\rangle = \sum_{n} c_n^k f_n^+ |0...0\rangle \tag{3.9}$$

We are going to obtain which are the c_n's that are the solution of the next eigenvalue equation:

$$\mathscr{H}|\psi\rangle = E|\psi\rangle \tag{3.10}$$

$$Ec_n^k = E_o c_n^k + J(c_{n+1}^k + c_{n-1}^k) \quad \text{for } n = 0,\ 1,\ 2,\ ...,\ N+1 \tag{3.11}$$

Applying boundary conditions:

$$\begin{cases} Ec_1^k = E_o c_1^k + Jc_2^k \ \ (c_o^k = 0) & \text{if } n = 1 \\ Ec_N^k = E_o c_N^k + Jc_{N-1}^k \ \ (c_{N+1}^k = 0) & \text{if } n = N \\ Ec_n^k = E_o c_n^k + J(c_{n+1}^k + c_{n-1}^k) & \text{if } 1 < n < N \end{cases} \tag{3.12}$$

In the case of translational invariance the momentum is conserved:

$$c_n^k = e^{ikn} + de^{-ikn} \tag{3.13}$$

[1] Where $\delta(k-k')$ is the Kronecker delta ($\delta(k-k') = 0$ if k is different to k' and 1 if they are equal)

[2] No periodic boundary conditions, the case of a finite chain of N sites.

Substituting this last relation we obtain:

$$\begin{aligned} Ec_n^k &= E_o c_n^k + J(c_{n+1}^k + c_{n-1}^k) = E_o c_n^k + J(e^{ik(n+1)} + de^{-ik(n+1)} + e^{ik(n-1)} + de^{-ik(n-1)}) = \\ &= E_o c_n^k + J[e^{ikn}(e^{ik} + e^{-ik}) + de^{-ikn}(e^{ik} + e^{-ik})] = \\ &= E_o c_n^k + 2J\left(\frac{e^{ik} + e^{-ik}}{2}\right) c_n^k = (E_o + 2J\cos(k)) c_n^k \end{aligned}$$

So, if we want to preserve the solution, we have to impose: $E = E_k = E_o + 2J\cos(k)$, as we have just said. Therefore, we have to check the solution of c_n in the limiting cases of $n = 1$ and $n = N$. In the first case:

$$\begin{gathered} 2J\cos(k)(e^{-ik} + de^{-ik}) = J(e^{i2k} + de^{-i2k}) \\ e^{i2k} + 1 + d + de^{-i2k} = e^{i2k} + de^{-i2k} \\ \longrightarrow \boxed{d = -1} \end{gathered}$$

Equivalently in the case of $n = N$:

$$\begin{gathered} (E_o + 2J\cos(k))(e^{ikN} - e^{-ikN}) = E_o(e^{ikN} - e^{-ikN}) + J(e^{ik(N-1)} - e^{i(N-1)k}) \\ \cdots \\ e^{ik(N+1)} - e^{-i(N+1)k} = 0 \longrightarrow \sin(k(N+1)) = 0 \end{gathered}$$

Therefore:

$$\boxed{k_n = \frac{\pi n'}{N+1} \equiv k_q n' \quad , \quad c_n^k = 2i\sin(k_n')}, \text{ where } n' = 0, \pm 1, \pm 2, \pm 3, ... \tag{3.14}$$

So, the eigenstate of our Hamiltonian $\mathscr{H}$ is:

$$\boxed{|\psi\rangle = C\sum_n \sin(k_q n') f_n^+ |0\ldots 0\rangle}, \text{ where } C \text{ is the normalization constant.} \tag{3.15}$$

Therefore, remembering equation (3.7) the energies corresponding to the eigenstates of the Hamiltonian (3.1) are:

$$E = \sum_{i=1}^{N} n_i(E_o + 2J\cos k_i), \text{ where } k_i = \frac{\pi n}{N+1} \text{ and } n = 0, \pm 1, \pm 2, \pm 3, ... \tag{3.16}$$

The factor n_i corresponds to the number of fermions (1 or 0) at the site "i".

As we have said it is much easier to work with spin operators instead of fermionic operators. Using the Jordan-Wigner relations that has been presented in the last chapter:

$$f_n^+ f_m = \sigma_n^+ e^{i\pi \sum_{l=1}^{n-1} \sigma_l^+ \sigma_l^-} e^{-i\pi \sum_{l=1}^{m-1} \sigma_l^+ \sigma_l^-} \sigma_m^- \longrightarrow \begin{cases} f_n^+ f_m = \sigma_n^+ e^{i\pi \sum_{l=m}^{n-1} \sigma_l^+ \sigma_l^-} \sigma_m^- & \text{if } n > m \\ f_n^+ f_n = \sigma_n^+ \sigma_n^- & \text{if } n = m \\ f_n^+ f_m = \sigma_n^+ e^{-i\pi \sum_{l=n}^{m-1} \sigma_l^+ \sigma_l^-} \sigma_m^- & \text{if } n < m \end{cases} \tag{3.17}$$

Substituting the above relations in Hamiltonian (3.1), we obtain its "spin-brother" Hamiltonian:

$$\mathscr{H} = E_o \sum_{n=1}^{N} \sigma_n^+ \sigma_n^- + J \sum_{n=1}^{N-1} \left(\sigma_n^+ e^{-i\pi \sigma_n^+ \sigma_n^-} \sigma_{n+1}^- + \sigma_{n+1}^+ e^{i\pi \sigma_n^+ \sigma_n} \sigma_n^- \right) \tag{3.18}$$

With the basis $\{|0\rangle, |1\rangle\}$ the operators $\sigma_n^+ \sigma_n^-,\ \sigma_n^+,\ \sigma_n^-$ are:

$$\sigma_n^+ = \begin{pmatrix} 0 & 0 \\ 1 & 0 \end{pmatrix} \qquad \sigma_n^- = \begin{pmatrix} 0 & 1 \\ 0 & 0 \end{pmatrix} \qquad \sigma_n^+ \sigma_n^- = \begin{pmatrix} 0 & 0 \\ 0 & 1 \end{pmatrix} \tag{3.19}$$

Hence the operator $e^{\pm i\pi \sigma_n^+ \sigma_n^-}$ is:

$$e^{\pm i\pi \sigma_n^+ \sigma_n^-} = \begin{pmatrix} 1 & 0 \\ 0 & e^{\pm i\pi} \end{pmatrix} \tag{3.20}$$

Therefore:

$$\sigma_n^+ e^{-i\pi \sigma_n^+ \sigma_n^-} = \begin{pmatrix} 0 & 0 \\ 1 & 0 \end{pmatrix} \begin{pmatrix} 1 & 0 \\ 0 & e^{-i\pi} \end{pmatrix} = \begin{pmatrix} 0 & 0 \\ 1 & 0 \end{pmatrix} = \sigma_n^+ \tag{3.21}$$

$$e^{+i\pi \sigma_n^+ \sigma_n^-} \sigma_n^- = \begin{pmatrix} 1 & 0 \\ 0 & e^{+i\pi} \end{pmatrix} \begin{pmatrix} 0 & 1 \\ 0 & 0 \end{pmatrix} = \begin{pmatrix} 0 & 1 \\ 0 & 0 \end{pmatrix} = \sigma_n^- \tag{3.22}$$

So, the tight-binding Hamiltonian of the fermions is equivalent to spin Hamiltonian:

$$\mathscr{H} = E_o \sum_{n=1}^{N} \sigma_n^+ \sigma_n^- + J \sum_{n=1}^{N-1} \left(\sigma_n^+ \sigma_{n+1}^- + \sigma_{n+1}^+ \sigma_n^- \right) \tag{3.23}$$

In other words the spin and fermionic operators are equivalent. So we are going to use the spin Hamiltonian in our algorithms to solve the scattering of one and two fermions.

3.1.1 Ground state energy - Tight Binding model

We already know how we can represent states and operators using MPS representation. In this section we are going to verify that our algorithm is correct. This program has been written using *MATLAB*. So, we are going to calculate the ground state energy using the imaginary time evolution method with simple initial states $|\psi(0)\rangle$. During the numerical calculus we have needed to truncate the size of the virtual indices between sites in our MPS representation of the state $|\psi(t+\delta t)\rangle$. This truncation will reduce this size to a fixed value which we will specify. Furthermore we will need to use the Suzuki-Trotter approximation to calculate the time evolution of our state preserving its MPS form. During this process we will commit some errors (due to the approximations) which will produce a change in the number of particles despite the fact that our Hamiltonian (3.23) preserves this number ($[H, \sigma_n^+ \sigma_n] = 0$). So we have to control this number to avoid a great increase. As we have seen we can use the spin Hamiltonian (3.23) and we use the following three initial states to verify that our program can obtain the ground state energy using imaginary time evolution:

$$|\Psi_1\rangle = \sigma_1^+ |0\rangle = |1000...\rangle\,; \quad |\Psi_2\rangle = \sigma_1^+\sigma_3^+ |0\rangle = |10100...\rangle\,; \quad |\Psi_3\rangle = \sigma_1^+\sigma_2^+\sigma_3^+ |0\rangle = |11100...\rangle \tag{3.24}$$

Notice that these states are spin states and we have said that we are going to study fermions. However in this part we have to notice that the Jordan-Wigner transformation preserves the number of excitations. Thus, the ground state of n spins excitations is the same as the ground state of n fermions. The parameters which we have used during each simulation are: $J = -1$, the value of truncation dimension $d = 5$; the order in Suzuki approximation order $= 3$, $E_o = 0$ and the chain length is $N = 5$ or 6 sites. On the other hand, remembering that ground state energy is: $E_{GS} = \sum_{k\in C}\left[E_o + 2J\cos(k_n)\right]$ and $k_n = \pi n/(N+1)$, $n = 1, 2, 3, ...$, where we sum over the $k's$ which minimize E_{GS}. We can calculate the theoretical value of E_{GS} in each case.

Firstly, $|\Psi_1\rangle = |1000...\rangle$, with $N = 5$. We only have one particle so the ground state energy is: $E_{GS} = -2\cos(\pi/(5+1)) \approx -1.732051$ If we compare this value with its equivalent calculated numerically $E_{GS}^{exp} = -1.732047$, they are equal up to the five digit. See *figure 3.2*.

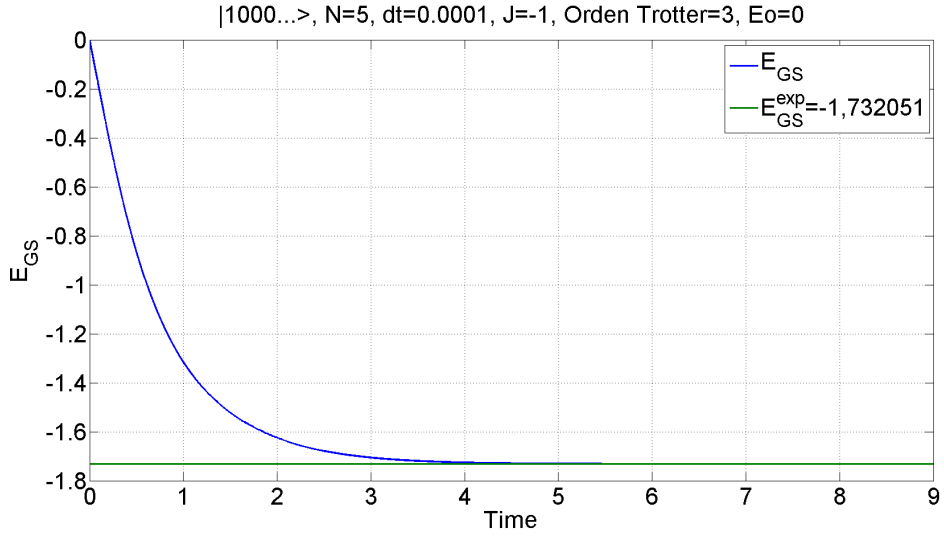

Figure 3.2: Simulation of the initial state $|\Psi_1\rangle = |1000...\rangle$ in a chain of length $N = 5$ to obtain the E_{GS} using imaginary time evolution. The analytic and numerical results are: $E_{GS} = -1.732051$ $E_{GS}^{exp} = -1.732047$

Secondly, $|\Psi_2\rangle = |1010...\rangle$, with $N = 6$. We have two particles now so the ground state energy is: $E_{GS} = -2(\cos(\pi/(6+1)) + \cos(2\pi/(6+1))) \approx -3.048917$ If we compare this value with its equivalent calculated numerically $E_{GS}^{exp} = -3.048907$, they have coincidence until the four digit. So, these results confirm the fact that we are dealing with fermions. On the contrary the ground state energy would have been $E_{GS} = -4(\cos(\pi/(6+1))$ instead of $E_{GS} = -2(\cos(\pi/(6+1)) + \cos(2\pi/(6+1)))$. See *figure 3.3*.

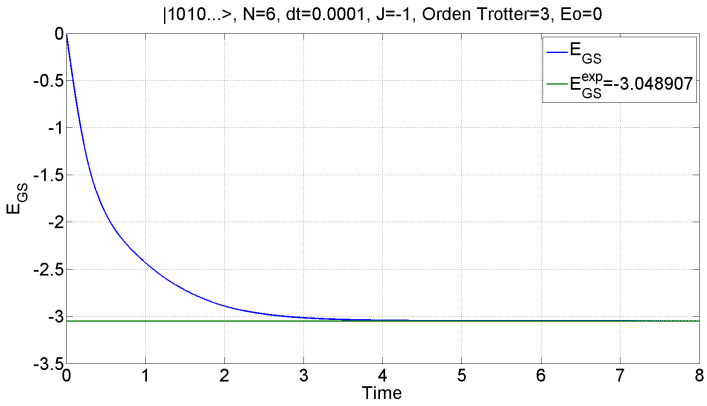

Figure 3.3: Simulation of the initial state $|\Psi_2\rangle = |1010...\rangle$ in a chain of length $N = 6$ to obtain the E_{GS} using imaginary time evolution. The analytic and numerical results are: $E_{GS} = -3.048917$ $E_{GS}^{exp} = -3.048907$

We can check the antisymmetry of the wave function calculating the components of the wave function: $c_{nm} = \langle 0|f_n^+ f_m^+|\Psi(t = t_{\text{final}})\rangle$ and checking that $c_{nm} = -c_{mn}$. So, as we can see in the next table the antisymmetry is conserved:

n/m	1	2	3	4	5	6
1	0	0,0528	0,1623	0,2706	0,3009	0,1909
2	-0,0528	0	0,1751	0,3688	0,4345	0,2965
3	-0,1623	-0,1751	0	0,2395	0,3583	0,2745
4	-0,2706	-0,3688	-0,2395	0	0,1902	0,1638
5	-0,3009	-0,4345	-0,3583	-0,1902	0	0,0525
6	-0,1909	-0,2965	-0,2745	-0,1637	-0,0525	0

Table 3.1: Table of the components c_{nm} of the wave function $|\Psi\rangle$ at the end of the simulation.

Thirdly, $|\Psi_3\rangle = |1110...\rangle$, with $N = 6$. We have three particles so the ground state energy is: $E_{GS} = -2(\cos(\pi/(6+1)) + \cos(2\pi/(6+1)) + \cos(3\pi/(6+1))) \approx -3.493959$ If we compare this value with its equivalent calculated numerically $E_{GS}^{exp} = -3.493959$, they are almost the same value. So with enough simulation time we can obtain very good results. See *figure 3.4*.

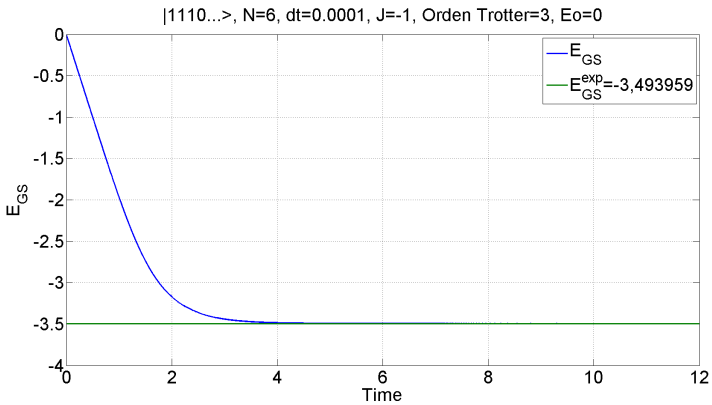

Figure 3.4: Simulation of the initial state $|\Psi_3\rangle = |1110...\rangle$ in a chain of length $N = 6$ to obtain the E_{GS} using imaginary time evolution. The analytic and numerical results are: $E_{GS} = -3.493959$ $E_{GS}^{exp} = -3.493959$

3.2 Single electron scattering

From now on, we are going to change the simple tight-binding model to study the electron transport through a Quantum Dot, (the model and results which we will check can be found in the article [4]), a region of the chain where the electrons interact with each other. So, remembering that we have a chain consisting on N "sites", we are going to situate our Quantum Dot in the middle of the chain to have enough space to propagate our electrons from one side to the other before they collide against the end of the chain. Therefore the Quantum Dot are the sites $(N/2, N/2+1)$. Up to now the hopping J_i between sites was equal independently of the position "i". However in the case which we are dealing with, our Quantum Dot is coupled with the rest of the chain through two different hopping constants $J_{N/2-1}$ and $J_{N/2+1}$. The rest of hopping constants are $J_i = -1$ where $i = 1,\ 2, ...,\ N-1,\ N$ except $i = N/2-1$ and $N/2+1$. Moreover, the energy E_o was equal in every site. Now, $E_o = 0$ except on sites $N/2$ $N/2+1$ where is equal to $E_o = e_{N/2}$ and $E_o = e_{N/2+1}$[3]. An interaction U between electrons exists, if the two sites which comprise the Quantum Dot are occupied by electrons. To sum up the Hamiltonian of the system is [4]:

$$H = H_{LR} + H_D + V \tag{3.25}$$

$$\begin{cases} H_{LR} = -\sum_{n=1}^{N-1}(f_n^+ f_{n+1}^+ + f_{n+1}^+ f_n) \quad \text{except } n = N/2-1,\ N/2 \text{ and } N/2+1 \\ H_D = e_{N/2} n_{N/2} + e_{N/2+1} n_{N/2+1} - (f_{N/2}^+ f_{N/2+1}^+ + f_{N/2+1}^+ f_{N/2}) + \dots \\ \cdots + J_{N/2-1}(f_{N/2-1}^+ f_{N/2}^+ + f_{N/2}^+ f_{N/2-1}) + J_{N/2+1}(f_{N/2+1}^+ f_{N/2+2}^+ + f_{N/2+2}^+ f_{N/2+1}) \\ V = U n_{N/2} n_{N/2+1} \end{cases} \tag{3.26}$$

Notice that $n_i = f_i^+ f_i$ is the number operator. Furthermore remembering the section about Jordan-Wigner, it is quite easy to show[4] that the spin Hamiltonian equivalent is the same, if we change the operator $f_n \to \sigma_n$.

But the title of this section is "single electron scattering". So, before the study of the two electron interaction, we are going to analyse the one electron scattering using the last Hamiltonian where we can get rid of the interaction term V. We have to remark that the electrons that we are going to consider along all the text are spinless electrons for simplicity. In the article [4], they give us reflection and transmission amplitudes, if the electron impacts from the right or from left on the Quantum Dot. In particular, for a particle incident from left or in other words with a momentum $k \in (0, \pi)$:

$$t_k = \frac{-2iJ_{N/2}J_{N/2+1}e^{-ik}\sin(k)}{(e_{N/2+1} - E_k - J_{N/2+1}^2 e^{ik})(e_{N/2} - E_k - J_{N/2}^2 e^{ik}) - 1} \tag{3.27}$$

$$r_k = \frac{1 - (e_{N/2+1} - E_k - J_{N/2+1}^2 e^{ik})(e_{N/2} - E_k - J_{N/2}^2 e^{-ik})}{(e_{N/2+1} - E_k - J_{N/2+1}^2 e^{ik})(e_{N/2} - E_k - J_{N/2+1}^2 e^{ik}) - 1} \tag{3.28}$$

where $E_k = -2\cos(k)$ is the energy of one particle with wave number $k \in (0, 2\pi)$

We are going to check these reflection and transmission amplitudes using our MSP method instead of the article [4] methods. Firstly, we build a wave packet of one electron with a mean momentum $K_o \in (0, \pi)$, a mean position on the chain X_o and variance σ:

$$|\Psi(t=0)\rangle = C\sum_{n=1}^{N} c_n f_n^+ |0\rangle\,, \text{ where } c_n = e^{-\frac{(n-X_o)^2}{2\sigma^2}} e^{-iK_o n} \text{ and C is the normalization constant.} \tag{3.29}$$

So, to calculate the transmission curve $|t_k|^2$ we need to follow some steps. 1) Firstly, we have to obtain the initial occupation $|c_k^{ini}|^2$ in the momentum space using the Fourier transform over our initial state $|\Psi(t=0)\rangle$ to get the $c_k's$. 2) Secondly, we simulate the propagation of our wave packet using Suzuki-Trotter decomposition to apply the evolution operator (to propagate our packet), MPS language to represent our state $\Psi(t)$ which codifies our wave packet of one electron and the truncation method to avoid matrices too big and reduce the memory necessities of the simulation. 3) Thirdly, after the scattering against the Quantum Dot, we obtain the the final occupation $|c_k^{fin}|^2$ in the momentum space using the Fourier transform over our final state $|\Psi(t=t_f)\rangle$. 4) We will divide the final occupation in the momentum space with the "transmission" $k \in (0, \pi)$ between the initial occupation in the momentum space of the initial packet to get the transmission curve: $|t_k|^2 = |c_k^{fin}|^2/|c_k^{ini}|^2$ with $k \in (0, \pi)$.

[3] See the Hamiltonian (3.23) to compare.

[4] See equation (3.17)

We can do that using two different methods:

3.2.1 First Method

In this method, we are going to be based on obtaining "point by point" of the transmission curve $|t_k|^2$. To do that we need a wave initial packet with a variance in the momentum space very small or in other words with a very well defined momentum k around K_0. So, due to the Heisenberg uncertainty principle, the variance σ in the position space has to be very large. Therefore, we will need a chain quite long to generate wide wave packets. When we will do this, we will be able to obtain $|t_{K_o}|^2$ at K_o, dividing $|c_k^{fin}|^2/|c_k^{ini}|^2$ where k coincides with the k of the peak of the initial occupation $|c_k^{ini}|^2$. Now, we are going to illustrate this method with an example, but firstly we will select the parameters of the theoretical curve $|t_k|^2$ which will make easier to obtain the curve $|t_k|^2$: $J_{N/2} = -1$, $J_{N/2+1} = -1$, $e_{N/2} = -0.6$ and $e_{N/2+1} = -0.6$:

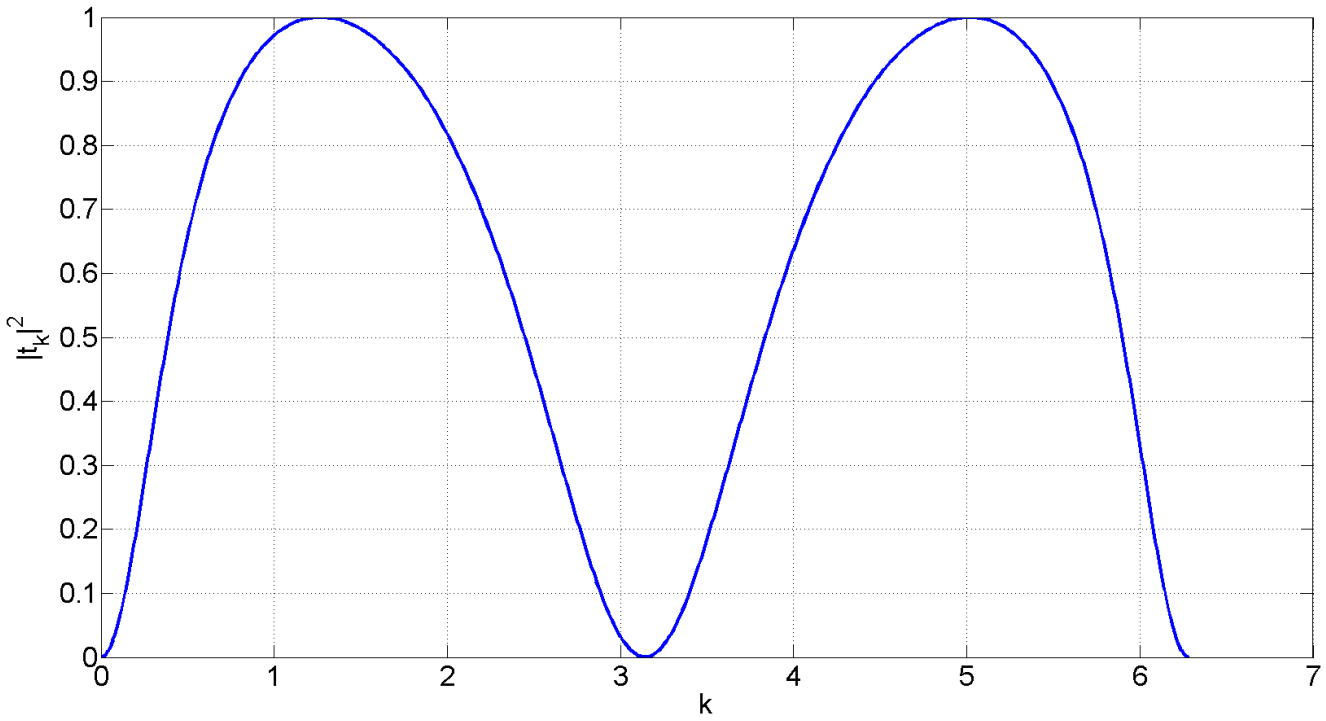

Figure 3.5: Transmission theoretical curve (see equation (3.27)) $|t_k|^2$ with parameters: $J_{N/2} = -1$, $J_{N/2+1} = -1$, $e_{N/2} = -0.6$ and $e_{N/2+1} = -0.6$

We are going to take the number of sites of our chain $N = 70$ with a initial packet with a variance $\sigma = 9.0$, a mean position $X_o = 18$ and a mean momentum $K_o = 2.1$:

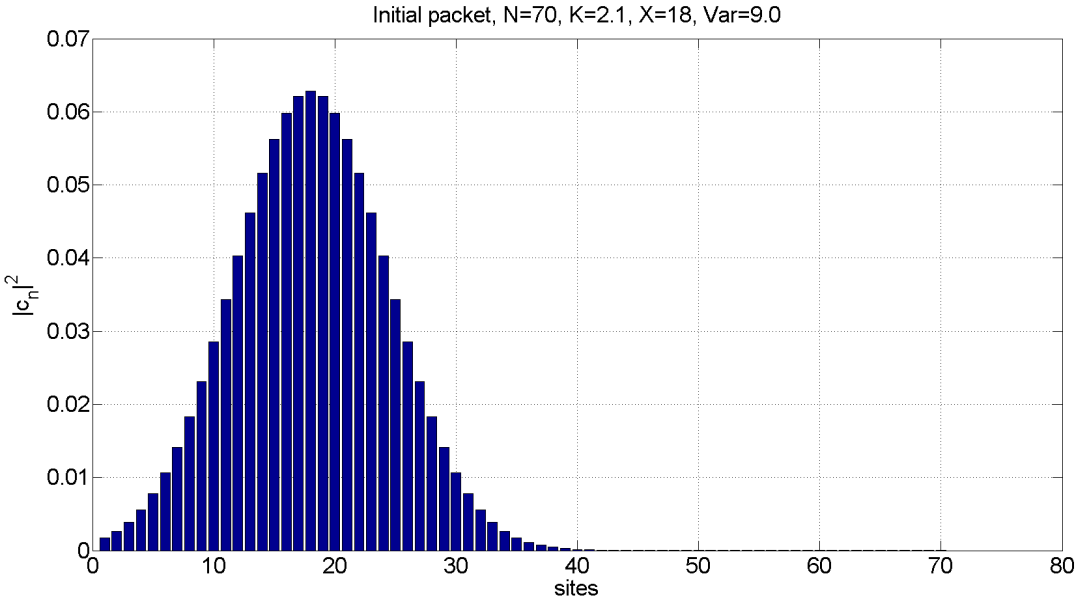

Figure 3.6: Initial packet in the position space with a variance $\sigma = 9.0$, a mean position $X_o = 18$ and a mean momentum $K_o = 2.1$

If we took the Fourier transform, the initial packet in the momentum space would be:

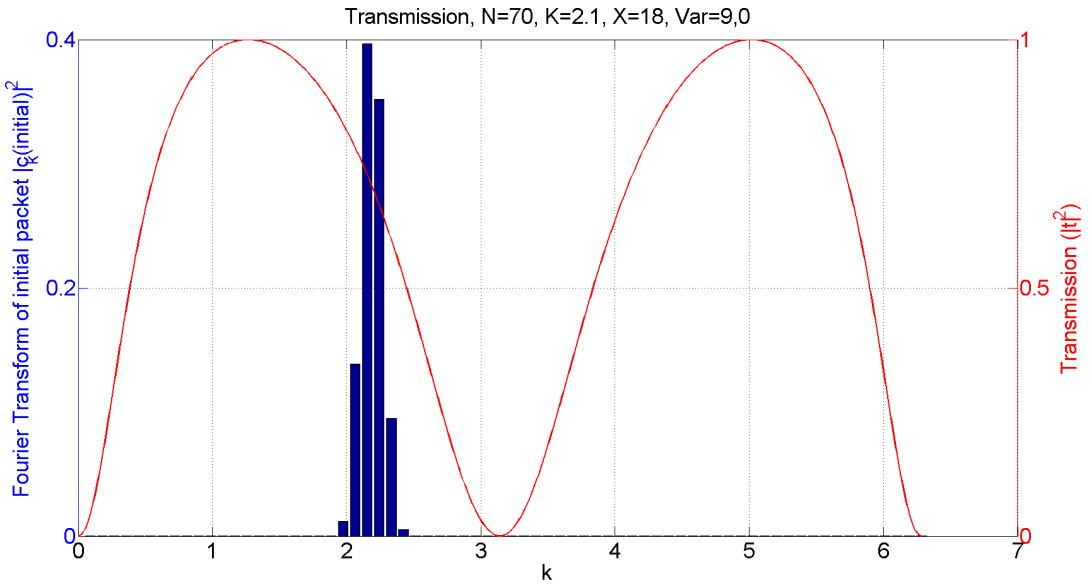

Figure 3.7: Initial packet in the momentum space with a variance $\sigma = 9.0$, a mean position $X_o = 18$ and a mean momentum $K_o = 2.1$

Once we have generated the initial state we are going to propagate it through the chain:

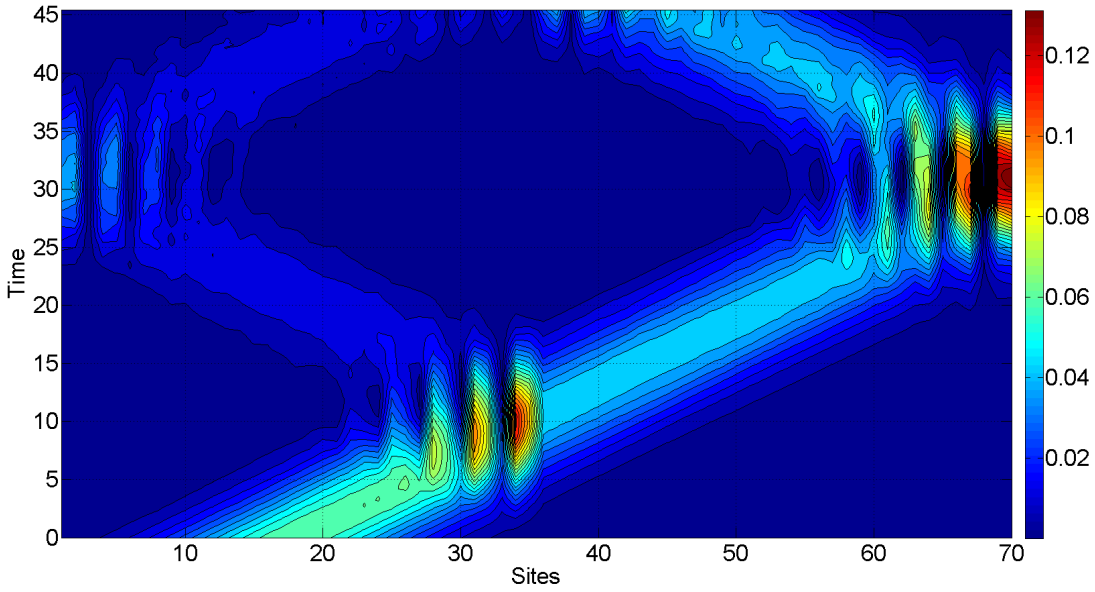

Figure 3.8: Propagation of the wave packet, the color represent higher or lower values of $|c_n|^2$ and the vertical axis is the time, the horizontal axis is the sites of the chain.

Another prove is to check that during the simulation the number of particles is preserved as our Hamiltonian imposes. So, if we see the evolution of number of particles in the *figure 3.9*, we see that the number of particles is not completely preserved due to the approximate method that we are using. Nevertheless, we have achieved that this increase of the number of particles is under control. As you can see the biggest increment in the number of particle respect to 1 particle is 0.35%.

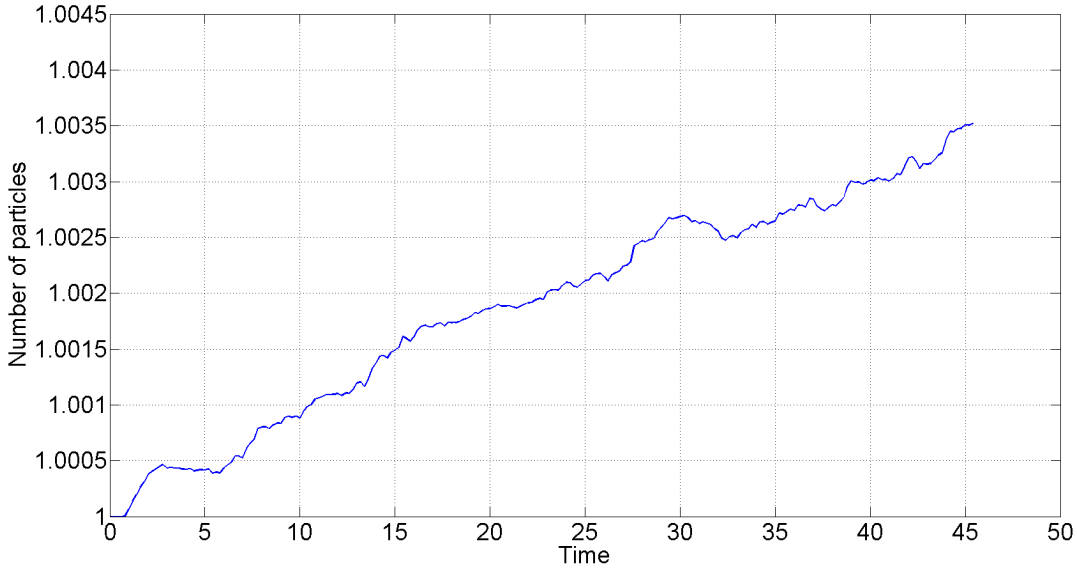

Figure 3.9: Evolution of the number of excitations (particles) during the simulation.

So, we are going to select $t = 20$ to calculate $|t_k|^2 = |c_k^{fin}|^2/|c_k^{ini}|^2$, before the wave packet collides with the end of the chain. We can compare $|t_k|^2$ with the initial packet $|c_k^{ini}|^2$ to choose the $|t_k|^2$ corresponding to the momentum K_o of the peak of $|c_k^{ini}|^2$:

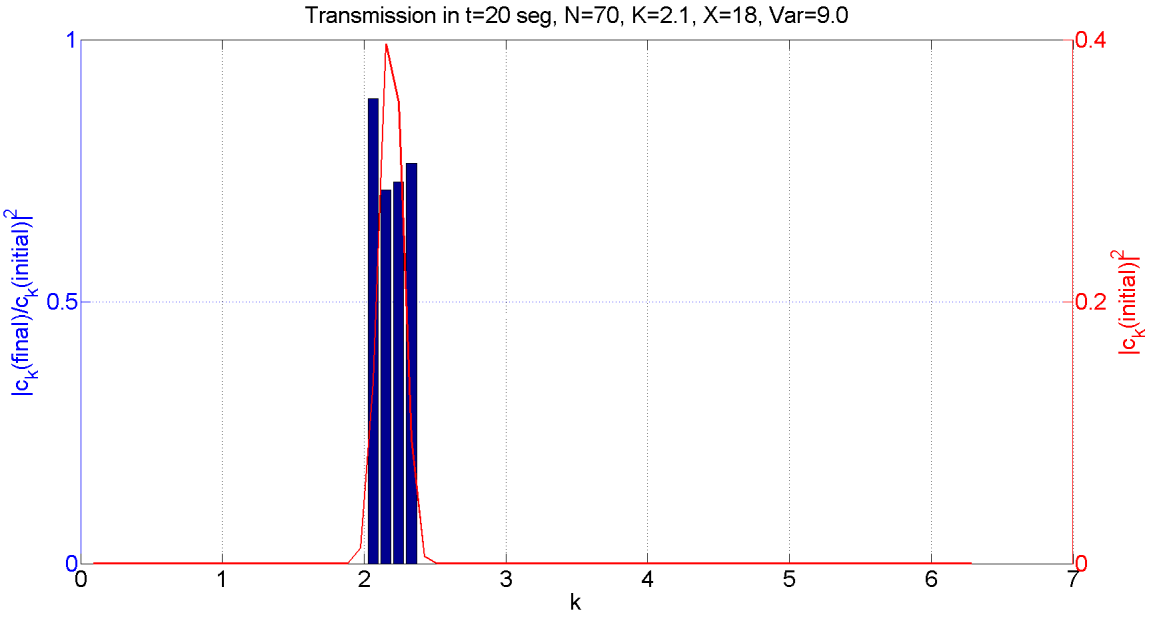

Figure 3.10: Comparison between $|t_k|^2 = |c_k^{fin}|^2/|c_k^{ini}|^2$ and $|c_k^{ini}|^2$

Therefore the K and $|t_K|^2$ selected are: $K = 2.1542$ and $|t_K|^2 = 0.7128$. Also, we can compare our calculus with the theoretical curve:

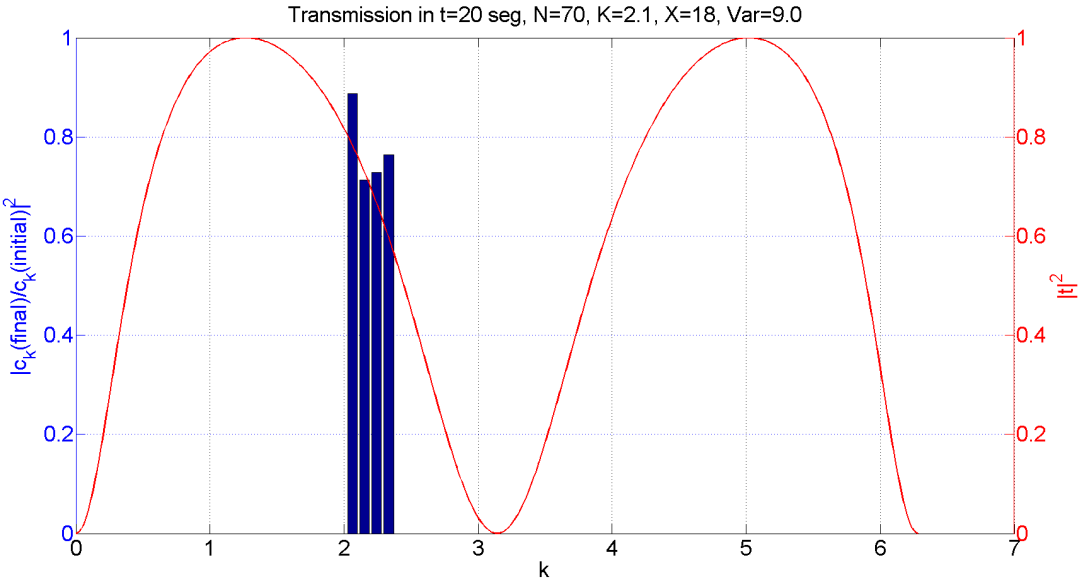

Figure 3.11: Comparison between calculated and theoretical $|t_k|^2$

Repeating this process for different values of the mean momentum K_o, we can obtain the different points of the transmision curve. In particular we have repeat this process for $K_o = 0.5,\ 0.9,\ 0.7,\ 1.3,\ 2.1$ and 2.5; obtaining:

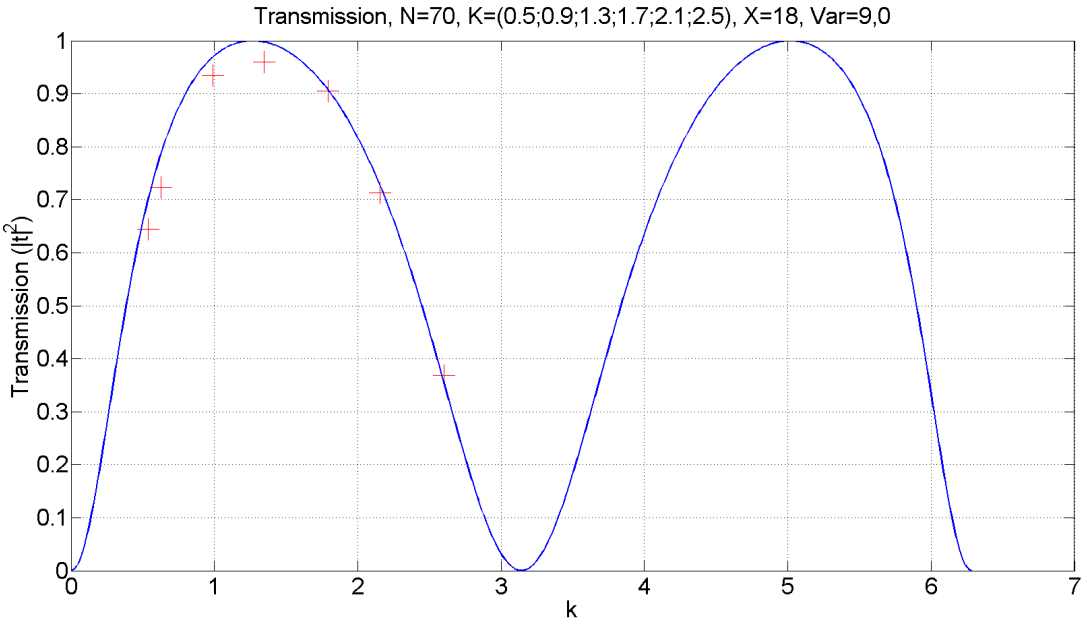

Figure 3.12: Comparison between calculated and theoretical $|t_k|^2$ for $K_o = 0.5,\ 0.9,\ 0.7,\ 1.3,\ 2.1$ and 2.5.

3.2.2 Second Method

In this second method instead of measuring each point of the transmission curve with a wave packet which a very well defined mean momentum K_o, we are going to do totally contrary. We will generate a wave packet with a very well defined position or a variance σ very small (we will take $\sigma = 2$ to illustrate the method in our case). This will allow us to have a very dispersive wave packet in the momentum space. So, instead of measure only one momentum of the transmission curve, we will measure $|t_k|^2$ around the mean momentum K_o of the wave packet. For example, (using the same transmission curve as in the last subsection, see *figure 3.5*) if we generate a wave packet with parameters: $N = 70$, $X_o = 18$, $\sigma = 2.0$ and $K_o = \pi/2$; in the position space:

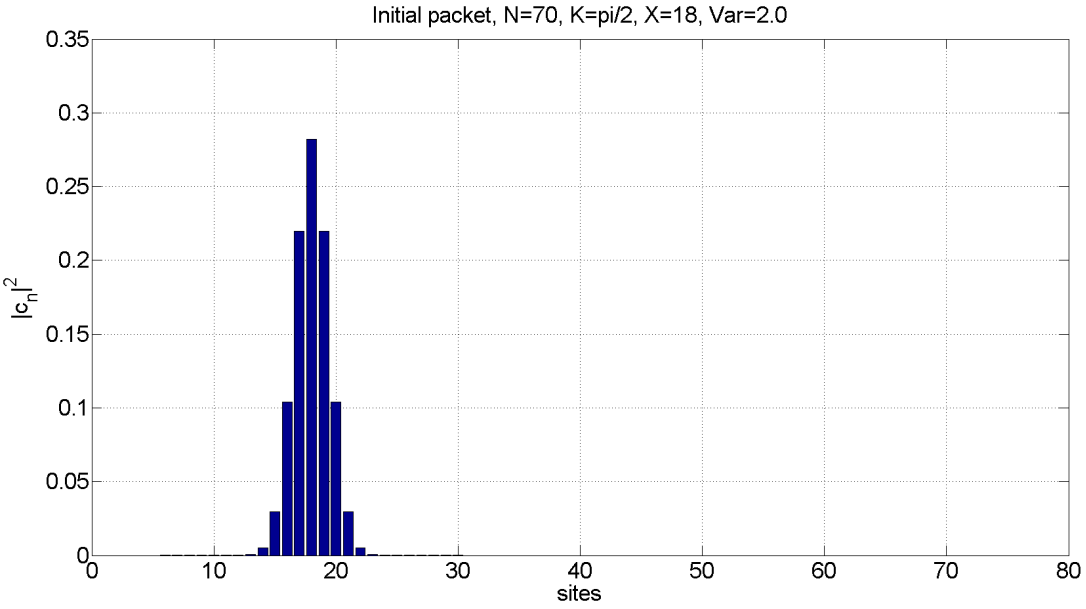

Figure 3.13: Initial wave packet in the position space with parameters: $N = 70$, $X_o = 18$, $\sigma = 2.0$ and $K_o = \pi/2$.

And in the momentum space:

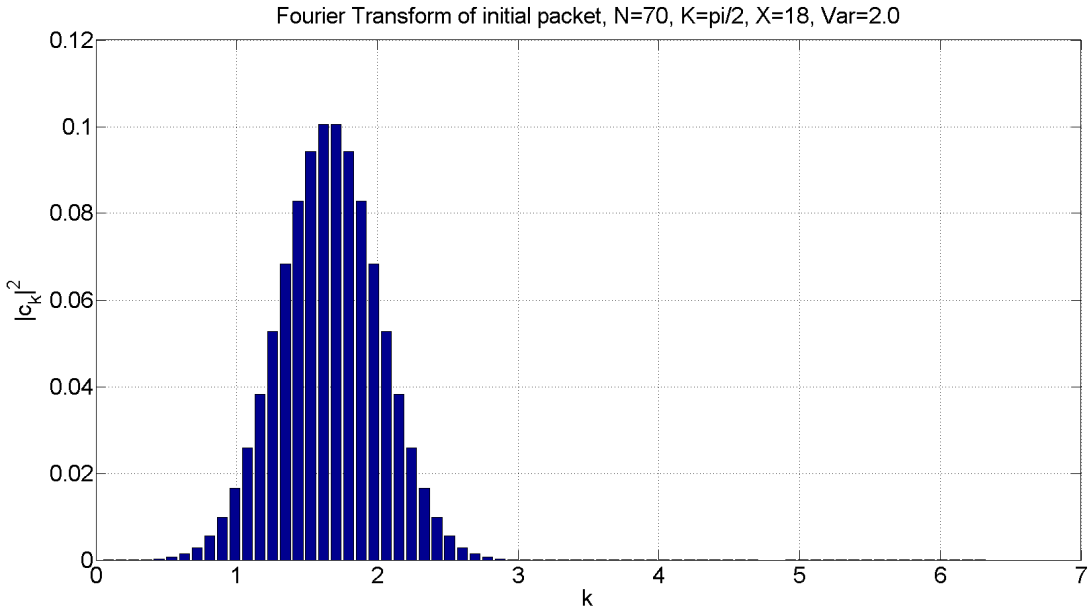

Figure 3.14: Initial wave packet in the momentum space with parameters: $N = 70$, $X_o = 18$, $\sigma = 2.0$ and $K_o = \pi/2$.

After that, we can propagate our wave packet until "the slowest"[5] momentum component collided against the Quantum Dot. Then, we will calculate $|t_k|^2 = |c_k^{fin}|^2/|c_k^{ini}|^2$ around the mean momentum $K_o = \pi/2$ whose limits are "the slowest" momentum selected. Therefore, the propagation of the wave packet is:

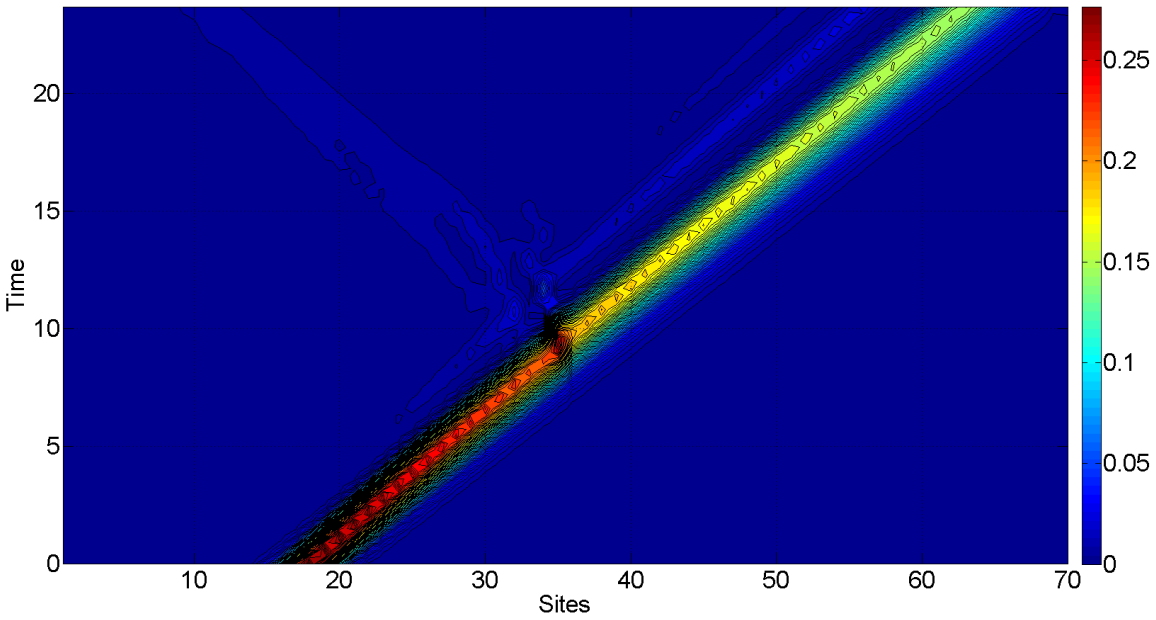

Figure 3.15: Propagation of the wave packet ith parameters: $N = 70$, $X_o = 18$, $\sigma = 2.0$ and $K_o = \pi/2$; the color represent higher or lower values of $|c_n|^2$, the vertical axis is the time and the horizontal axis is the sites of the chain.

[5]We do not strictly take the slowest component because of the fact its velocity is zero. So, we will select a very slow component but not the slowest.

And finally the $|t_k|^2 = |c_k^{fin}|^2/|c_k^{ini}|^2$ around the mean momentum $K_o = \pi/2$ in comparison with the theoretical curve is:

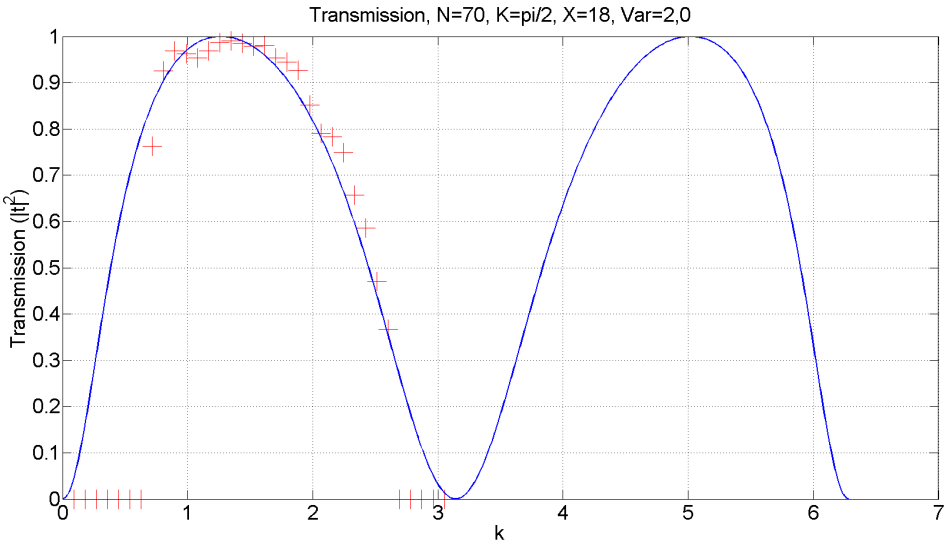

Figure 3.16: The theoretical and computed values around mean momentum K_o of the transmission curve $|t_k|^2$. The zero values of the points have been fixed by hand, because in these cases the error in the measure was very remarkable.

So, as you have just seen this alternative method is much more efficient than the other. As we will see in the next section the first method is usefull for problems with more than two electrons. Once we have done this, we can calculate the same for more values of K_o to cover all the transmission curve with two additional simulations[6]. In particular, we have repeated the process for the mean momentums: $K_o = \pi/4$ and $3\pi/4$ obtaining the *figure 3.17* with all measures of the three mean momentums.

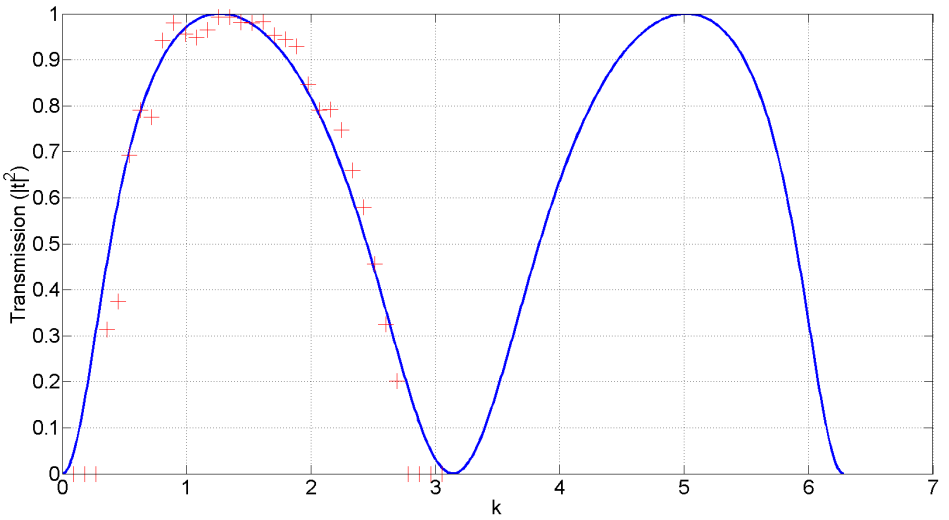

Figure 3.17: The theoretical and computed values of the transmission curve $|t_k|^2$. We have included the measures with the packet of mean momentums: $K_o = \pi/4$, $\pi/2$ and $3\pi/4$. The zero values of the points have been fixed by hand, because in these cases the error in the measure was very remarkable.

[6]Due to the symmetry of the curve $|t_k|^2$

3.3 Two electron scattering

We have just reproduced some results of [4] in the case of one particle scattering against the Quantum Dot. Before dealing with the scattering of two electrons against the Quantum Dot, we only have to check one last thing. The free propagation of two electrons through the one dimensional or in other words the tight-binding model without the Quantum Dot. We have used a chain of $N = 40$ sites, with two wave packets at $X_o(1) = 8$ and $X_o(2) = 24$ with a mean momentum $K_o = \pi/2$ (the other technical parameters are: dimension of truncation is equal to 5, the time step is $\delta t = 0.1$ and the order of Suzuki-Trotter approximation is 3). We can see in the *figure 3.16* that the behaviour is the expected. The two ideal collisions against the end of our one dimensional lattice.

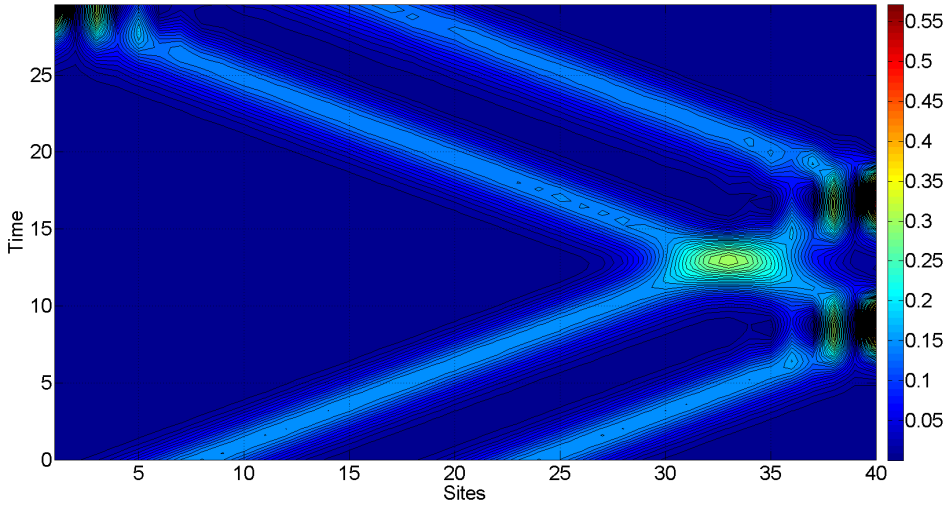

Figure 3.18: Free propagation of two electrons with mean momentum $K_o = \pi/2$ and variance $\sigma = 3.5$ in a one-dimensional lattice of $N = 40$ sites.

But a very important prove of the good running of the algorithm is the preserve of the number of particles, since our Hamiltonian guarantees this preservation as we have said in last sections. This condition is fulfilled quite good as we can see in the *figure 3.16*. Since the maximum deviation error respect to the theoretical value of two particles is 0.015%.

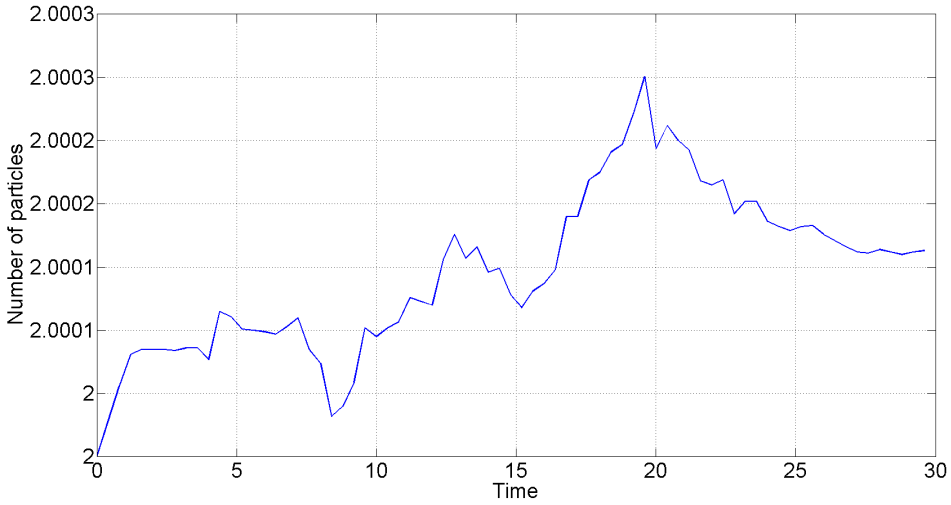

Figure 3.19: Evolution of the number of excitations (particles) during the simulation.

So, we have now all the necessary tools to be able to reproduce some results of the article [4] about the scattering and interaction of two particles in the Quantum Dot. One that we would have liked to reproduce is the resonance phenomenon of the transmission through the Quantum Dot. In [4] they observed that for a value of $U = 1.45$ of the interaction parameter, it produced a great increased in the electronic current through the Quantum Dot if we eliminate the equivalent current without the interaction term V in the Hamiltonian (3.25). However the curve presented in the article (*figure 1* of [4]) have a peak with a variance very small (in energy units) of the order of $\Delta U \sim 0.125$.

So, we need to use the first method presented in the last section. This implies that we need a wave packet with a very lager variance in the position space in order to measure the transmission in that narrow window of energies with $\Delta U \leq 0.125$. Therefore, we would need very long one-dimensional lattice to generate these so dispersive wave packets (in the position space).

If we take into account al that I have just said. We have estimated that we will need one-dimensional lattices with a length equal or larger than $N = 200$. So, we will need not only more memory to generate the two wave packets in a longer chain but also we would require bigger simulation times due to the length of the lattice. So, we would have need more powerful computers than a simple PC, a task reverved to future projects. So, we would go beyond the article [4], since we could have obtained results related with the propagation and scattering of more than two electrons: three, four electrons...

Chapter 4

Conclusions

We started the beginning of our text discussing the aptitude of the MPS scheme to solve a many-body problem, and represent our states and operators. However, the aim of this work has been to prove the validity of an algorithm based in the MPS representation to study the scattering and electronic interaction in a limited region of our one-dimensional lattice known as Quantum Dot, using a tight-binding model [4]. Obtaining, at the end, a method capable to study the scattering of more than only two electrons against our Quantum Dot.

In order to develop our algorithm has been necessary the use of many different tools presented during chapter 2. The Suzuki-Trotter approximation permitted us to build an evolution operator easily applicable to our MPS scheme of our initial state and therefore obtain its propagation through our lattice. Then, the imaginary time evolution has allowed to obtain in chapter 3 the ground state energy for the cases of one, two and three excitations in short chains. After that, the Jordan-Wigner equivalence allowed us to find a spin equivalent to our fermionic Hamiltonians and use the spin operators much easier of dealing with. Finally we introduced the truncation, a crucial method, since this method reduce the necessary memory during the simulation due to the reduction of the size of the matrices.

After this introductory chapter, we have been checking several aspects of the scattering and propagation of one and two electrons through the one-dimensional lattice. Firstly, we obtained the diagonalization of our tight-bingding Hamiltonian and the analytic form of the ground state energy. Thereupon, we got the ground state energy for the cases of one, two and three excitations in short chains using imaginary time evolution, as we have said. In this section, we could confirm the fermionic behaviour of our particles, since each level of energy could only be occupied by one electron or zero, and we could compare the numerical with analytical results. Also, the algorithm preserved the antisymmetry of the wave function, a characteristic property of the fermionic particles.

Then, we started with the studying of the scattering of one electron using now the tight-binding Hamiltonian of [4]. We reproduce the transmission curve $|t_k|^2$ [4] using two different methods; both to gain further confidence on the method and depending on the situation one is more efficient than the other. So, our algorithm is capable to reproduce correctly the scattering of one electron. Once, we arrived to that point we could have continued studying the scattering of two electrons and their interaction in the Quantum Dot zone. Thus, we could have reproduced the resonance process presented in [4], calculating the different transmission amplitudes for each U (interaction parameter) value. To sum up, we can say now that we have obtained a method capable to reproduce in future projects the scattering processes with two electrons. Apart from that it is perfectly possible to use this method to navigate beyond the study presented in the article in connection with resonance phenomenon. We could simulate the cases of more than two electrons, three, four... or introduce some sophistications to model as using electrons with spins instead of spinless electrons.

Bibliography

[1] Zhihong Chen, Yu-Ming Lin, Michael J. Rooks and Phaedon Avouris; Physica E: Low-dimensional Systems and Nanostructures, Vol. 40/2, 228-232 (2007); *graphene Nano-Ribbon Electronics*

[2] Xinran Wang, Yijian Ouyang, Xiaolin Li, Hailiang Wang, Jing Guo and Hongjie Dai; arXiv:0803.3464; *Room Temperature All Semiconducting sub-10nm graphene Nanoribbon Field-Effect Transistors*

[3] Y. Hancock, A. Uppstu, K. Saloriutta, A. Harju and M. J. Puska; Physical Review B 81, 245402 (2010); *Generalized tight-binding transport model for graphene nanoribbon-based systems*

[4] Dibyendu Roy, Abhiram Soori, Diptiman Sen and Abhisshek Dhar; Physical Review B 80, 075302 (2009); *Nonequilibrium charge transport in an interacting open system: two-particle resonance and current asymetry*

[5] Román Orús, arXiv:1306.2164v1 [cond-mat.str-el]; *A practical introduction to tensor networks: Matrix Product States and Projected Entanglement Pair States*; Intitute of Physics, Johannes Gutenberg University.

[6] J. Ignacio Cirac and Frank Verstraete; Journal of Physics A: Mathematical and Theoretical, 42 (2009); *Renormalization and tensor product states in spin chains and lattices*

[7] J. Nagamatsu, N. Nakagawa, T. Muranaka, Y. Zenitani, J. Akimitsu; Nature 410 (6824) pp63-64 (2001); *Superconductivity at 39K in magnesium diboride*

[8] A. Altand and B. Simons; Cambridge University Press, pp. 58, ISBN: 978-0-52-176975-4 (2006); *Condensed Matter Field Theory*

[9] C. Eckart, G. Young, Psychometrika 1 (3): 211-8 (1936) ; *The approximation of one matrix by another of lower rank*

[10] Michael M. Wolf, Frank Verstraete, Matthew B. Hastings and J. Ignacion Cirac; Phys. Rev. Lett. 100, 070502 (2008); *Area Laws in Quantum Systems: Mutual Information and Correlations*

[11] Guifré Vidal; Phys. Rev. Lett. 91, 147902 (2003); *Efficient classical simulation of slightly entangled quantum computations*

[12] Anirban Pathak ; Taylor & Francis, pp. 92, ISBN: 978-1-46-651791-2 (2013); *Elements of Quantum Computation and Quantum Communication*

[13] Charles H. Bennett, Herbert J. Bernstein, Sandu Popescu and Benjamin Schumacher; Phys. Rev. A 53, 2046-2052 (1996); *Concentrating Partial Entanglement by Local Operations*

[14] Ian P. McCulloch, Journal of Statistical Mechanics: Theory and Experiment, P10014 (2007), *From density-matrix renormalization group to matrix product states*

[15] Juan José García-Ripoll, New Journal of Physics 8 (2006) 305, *Time evolution of Matrix Product States*

[16] Eduardo Sánchez Burillo; Repositorio Institucional de Documentos de UNIZAR (`http://zaguan.unizar.es/record/11469?ln=es`) ; *Teoría de scattering de n fotones con m qubits en guías de onda*